View metadata, citation and similar papers at core.ac.uk

brought to you by CORE

provided by DigitalCommons@URI

Masthead Logo

University of Rhode Island
DigitalCommons@URI

Chemistry Faculty Publications

Chemistry

2017

Reversible Graphite Anode Cycling with PC-Based Electrolytes Enabled by Added Sulfur Trioxide Complexes

Julien Demeaux

Yingnan Dong

See next page for additional authors

Creative Commons License
Creative Commons License
This work is licensed under a Creative Commons Attribution 4.0 License.

Follow this and additional works at: https://digitalcommons.uri.edu/chm_facpubs

Citation/Publisher Attribution

Demeaux, J., Dong, Y., & Lucht, B. L. (2017). Reversible Graphite Anode Cycling with PC-Based Electrolytes Enabled by Added Sulfur Trioxide Complexes. *J. Electrochem. Soc., 164*(7), A1352-A1360. doi: 10.1149/2.0171707jes
Available at: http://dx.doi.org/10.1149/2.0171707jes

This Article is brought to you for free and open access by the Chemistry at DigitalCommons@URI. It has been accepted for inclusion in Chemistry Faculty Publications by an authorized administrator of DigitalCommons@URI. For more information, please contact digitalcommons@etal.uri.edu.

Authors
Julien Demeaux, Yingnan Dong, and Brett L. Lucht

This article is available at DigitalCommons@URI: https://digitalcommons.uri.edu/chm_facpubs/124

Reversible Graphite Anode Cycling with PC-Based Electrolytes Enabled by Added Sulfur Trioxide Complexes

Julien Demeaux, Yingnan Dong, and Brett L. Lucht*,z

Department of Chemistry, University of Rhode Island, Kingston, Rhode Island 02881, USA

Pyridine sulfur trioxide ($PyrSO_3$), trimethyl amine sulfur trioxide (Me_3NSO_3), and triethyl amine sulfur trioxide (Et_3NSO_3) complexes have been investigated as electrolyte additives for lithium ion batteries. Incorporation of 0.5 to 2.0% of the SO_3 complexes into a PC/EMC (1:1 v/v) 1 M $LiPF_6$ baseline electrolyte affords reversible cycling of graphite anodes confirming generation of a stable Solid Electrolyte Interphase (SEI). Good cycling performance is observed for graphite/$LiNi_{0.5}Mn_{1.5}O_4$ cells cycled to high potential (4.8 V vs Li) containing PC based electrolyte with added SO_3 complexes. Ex-situ surface analysis via X-ray Photoelectron Spectroscopy (XPS) of the anodes reveals SO_3 complex reduction on the surface of the graphite anode generates a sulfur-based SEI containing sulfites, sulfide, and sulfate species. The presence of the sulfur containing species is likely critical for the stability of the SEI. Ex-situ XPS analyses of the $LiNi_{0.5}Mn_{1.5}O_4$ cathodes suggest that reaction of Me_3NSO_3 or Et_3NSO_3 complexes at high potential result in the generation of a stable passivation layer which affords good capacity retention and coulombic efficiency.
© The Author(s) 2017. Published by ECS. This is an open access article distributed under the terms of the Creative Commons Attribution 4.0 License (CC BY, http://creativecommons.org/licenses/by/4.0/), which permits unrestricted reuse of the work in any medium, provided the original work is properly cited. [DOI: 10.1149/2.0171707jes] All rights reserved.

Manuscript submitted March 20, 2017; revised manuscript received April 18, 2017. Published April 29, 2017.

The standard anode material in most commercial lithium ion batteries is graphite due to good specific capacity, low volumetric expansion upon Li^+ intercalation, relatively flat potential profile, excellent cyclability, and low cost. However, the reduction potential of lithiated graphite is below the stability window of most organic solvents and thus requires the formation of a Solid Electrolyte Interphase (SEI).[1,2] Only a few electrolytes result in the formation of a stable SEI on graphite and most of these electrolytes include ethylene carbonate (EC) due to the critical role of EC in SEI formation.[3] An alternative solvent, propylene carbonate (PC), has been already extensively studied for use in lithium-ion batteries due to its favorable physical properties: high relative permittivity ($\varepsilon = 64.96$) and wide operating temperature range (mp = -55°C, bp = 240°C).[2] However, reduction of PC does not generate a stable SEI on graphite leading to continuous electrolyte reduction and graphite exfoliation. In addition, EC has recently been reported to have high reactivity with the surface of cathodes operating at high potential.[4,5]

In order to use PC based electrolytes an electrolyte additive is required to assist with SEI formation.[6] One type of additive which frequently stabilizes the SEI are sulfur-based compounds,[7] including SO_2,[8,9] CS_2,[10] polysulfides S_x^{2-},[11,12] cyclic alkyl sulfites, such as ethylene sulfite,[13] propylene sulfite,[14] and aryl sulfites,[14] propane sultone,[15] butyl sultone,[16] functionalized sulfones,[17] and sulfates.[18] All of these sulfur compounds are soluble in the organic electrolytes, but anodic unstable at high potential.[6] Propane sultone is one of the most widely investigated sulfur based additives and has been reported to improve Li^+ conduction in the anode SEI. However, due to toxicity concerns there is an interest in finding an alternative to PS. Previously reported ex-situ surface analysis of graphite anodes cycled with PS suggests that the primary reduction product of PS is lithium propane sulfonate (RSO_3Li).[19,20] In an effort to develop Additives for Designed Surface Modification (ADSM),[21] novel SO_3 based additives have been developed to generate similar reduction products to the lithium alkyl sulfonates generated from the reduction of PS.

Sulfur trioxide complexes, have been investigated as novel additives for PC/EMC (ethyl methyl carbonate) 1 M $LiPF_6$ electrolyte. The chemical structures of pyridine sulfur trioxide ($PyrSO_3$),[22] trimethyl amine sulfur trioxide (Me_3NSO_3), and triethyl amine sulfur trioxide (Et_3NSO_3) complexes are provided in Figure 1.

The complexes are bifunctional and combine the advantages of both a Lewis base (pyridine, trimethyl amine, or triethylamine) which inhibits $LiPF_6$ decomposition[23] and an anode film forming agent (SO_3) which improves cycling stability on graphite through modification of the SEI via incorporation of the SO_3 reduction products.[11,22] Coin cells composed of Graphite/Li and $LiNi_{0.5}Mn_{1.5}O_4$/Graphite have been prepared and cycled with the PC-based electrolyte containing the SO_3 complexes in order to study the ability of the additives to generate passivation layers on either the graphite anode and/or the high voltage spinel cathode. A systematic XPS study conducted after cycling shows that the surface chemistry of both electrodes are modified with the added SO_3 complexes.

Experimental

The levels of HOMO and LUMO energies were performed on isolated EMC, PC, $PyrSO_3$, Me_3NSO_3, and Et_3NSO_3 in the gas phase using the Gaussian 03 package.[24] HOMO and LUMO energies were obtained with the B3LYP/6-311+G(2d,p) basis set.

Coin cells were assembled with 2032-type coin cell parts from MTI, including SUS 304 Al- clad cases, SUS 316L caps, PP gaskets, disk spacers of 15.5 mm diameter and 1.0 mm of thickness, and wave springs of 15 mm diameter and 1.4 mm of thickness.

The cells were built with commercially coated electrodes: $LiNi_{0.5}Mn_{1.5}O_4$ (d = 14.7 mm) and graphite anode (d = 15.0 mm), a piece of Whatman glass fiber (d = 19 mm) with 80 μL of electrolyte in an Argon-filled glove box. The water content was less than 0.1 ppm. The baseline electrolyte was 1.0 M $LiPF_6$ in PC/EMC (1/1 v/v). Battery grade carbonate solvents and lithium hexafluorophosphate ($LiPF_6$) were obtained from BASF. Pyridine (98%), trimethylamine (95%), and triethylamine (95%) sulfur trioxide complexes were obtained from Sigma Aldrich and added as 2.0%, 1.0%, or 0.5% weight percent of the total mass of electrolyte, all three additives can be dissolved in baseline electrolyte easily up to 2%.

Cells were cycled at 25°C at the C/5 rate on Arbin Instruments potentiostats following a CC-CV protocol. A constant current (CC) charge was applied to reach the desired potential. This potential was maintained (CV) until the current decreased down to 10% of the

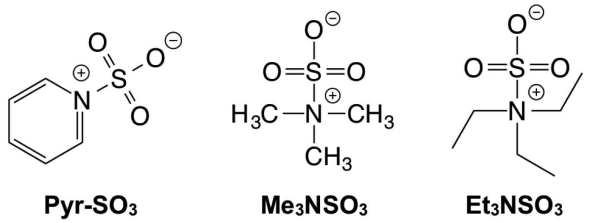

Figure 1. Sulfur trioxide complexes used as additives in the PC/EMC (1/1 v/v) 1 M $LiPF_6$ baseline electrolyte.

*Electrochemical Society Member.
zE-mail: blucht@chm.uri.edu

Downloaded on 2019-04-18 to IP 131.128.197.122 address. Redistribution subject to ECS terms of use (see ecsdl.org/site/terms_use) unless CC License in place (see abstract).

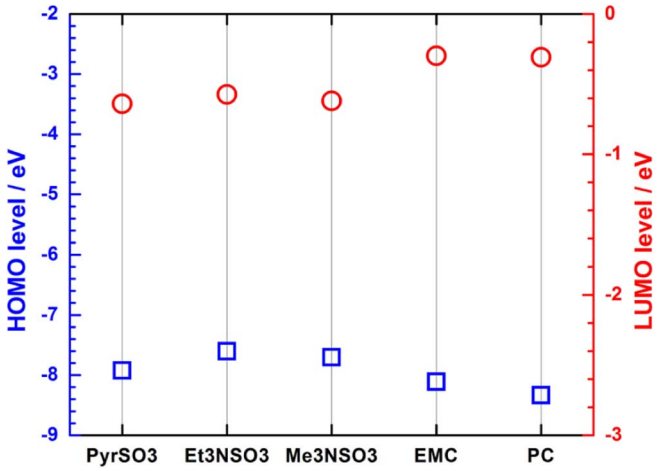

Figure 2. HOMO and LUMO levels of $PyrSO_3$, Et_3NSO_3, and Me_3NSO_3 calculated by DFT (Gaussian 03) and the B3LYP/6-311+G(2d,p) basis set.

applied charging current for a maximum duration of 1 hour. The temperature was controlled with a Fisher Scientific Isotemp Incubator. Formation cycling of graphite cells was as follows: 5 cycles, 1 cycle at C/20 rate, 2 cycles at C/10, and 2 cycles at C/5 rate at 25°C. The remaining cycles were performed at a cycling rate of C/5. Cycling was conducted in the 4.80–3.30 V potential range in the case of $LiNi_{0.5}Mn_{1.5}O_4$/graphite cells.

XPS measurements were carried out using a ThermoFisher K-Alpha spectrometer, under focused monochromatised Al Kα radiation ($h\nu = 1486.6$ eV). Cells were disassembled in the glove box and electrode samples were rinsed 3 times (3×500 µL) with anhydrous DMC and dried under vacuum at room temperature for 10 minutes. A vacuum transfer vessel (provided by ThermoFisher) was used to avoid any contact with air/moisture. Peaks were recorded with constant pass energy of 50 eV with energy resolution of 50 meV and charge neutralization. The peak positions and areas were optimized by a weighted least squares fitting method using 70% Gaussian, 30% Lorentzian line shapes using the Avantage (ThermoFisher) software.

Results and Discussion

HOMO and LUMO energy levels determined by DFT calculations.—HOMO and LUMO energy levels are calculated by DFT using the B3LYP/6-311+G(2d,p) basis set to evaluate relative oxidation and reduction potentials of sulfur trioxide complexes, as compared to EMC and PC. Results of HOMO and LUMO levels are depicted in Figure 2.

As seen from Figure 2, the HOMO levels of $PyrSO_3$, Et_3NSO_3, and Me_3NSO_3 are higher than the HOMO levels of EMC and PC. This suggests that the sulfur trioxide complexes are more easily oxidized than EMC or PC. Oxidation at high potential could result in modification and passivation of the cathode surface.

LUMO levels of the three sulfur trioxide complexes are similar. They have lower LUMO energies than EMC and PC (Figure 2), suggesting that they are more easily reduced than the carbonates. Their reduction at low potential should modify the SEI on graphite at low potential.

Graphite half-cells.—*Electrochemical cycling.*—Since $PyrSO_3$, Et_3NSO_3, and Me_3NSO_3 are the theoretically more easily reduced than PC and EMC and the reduction products are likely similar to the reduction products of PS as described above, they are potentially interesting additives for surface modification of the graphite anode. One method to investigate efficient passivation of graphite is to incorporate the additive into a PC-based electrolyte. It is well known that PC is continuously reduced at 0.8 V vs. Li/Li^+ with little Li^+ insertion and significant exfoliation of the graphite.[25]

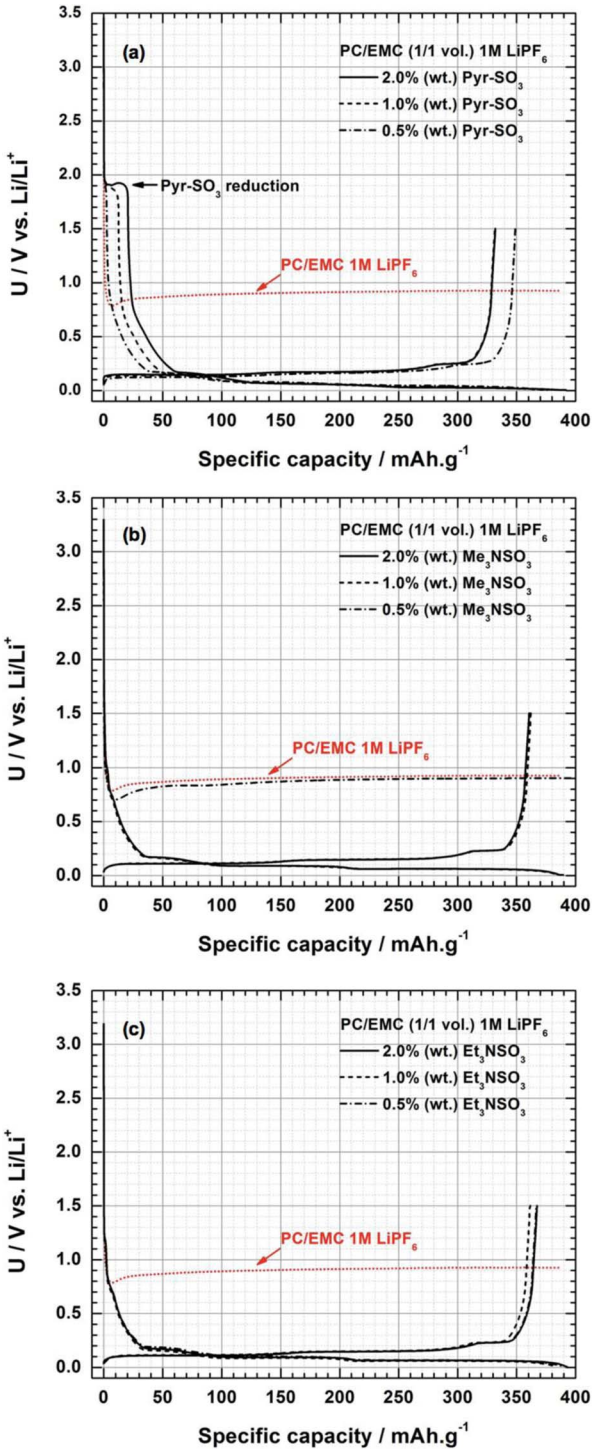

Figure 3. Voltage profile of the first cycle of Graphite/Li half-cells at 25°C (C/20, cutoff limits of 0.005 V vs. Li/Li^+ and 1.5 V vs. Li/Li^+) using PC/EMC (1/1 vol.) $LiPF_6$ 1 M as the baseline electrolyte with the (a) $PyrSO_3$, (b) Me_3NSO_3, and (c) Et_3NSO_3 additives (concentrations of 2.0%, 1.0%, and 0.5% (wt)).

The first cycle of Graphite/Li cells with PC based electrolyte containing added $PyrSO_3$, Me_3NSO_3, or Et_3NSO_3 is presented in Figure 3. Continuous electrolyte reduction is observed for the baseline PC electrolyte at 0.8 V vs. Li/Li^+ due to a lack of passivation of the graphite electrode (Figures 3a, 3b, and 3c).[26]

Incorporation of $PyrSO_3$ to the baseline formulation results in the appearance of a new shoulder at 1.9 V vs. Li/Li^+. The capacity of

Downloaded on 2019-04-18 to IP 131.128.197.122 address. Redistribution subject to ECS terms of use (see ecsdl.org/site/terms_use) unless CC License in place (see abstract).

Table I. Relative atomic percentage (%) of selected elements at the surface of the graphite electrodes after 1 cycle in Graphite/Li cells at 25°C. Relative atomic concentration of elements present at the fresh graphite electrode is also added for comparison.

Additive concentration		C 1s	F 1s	O 1s	Li 1s	S 2p	N 1s	P 2p
Fresh graphite		85	-	15	-	-	-	-
$PyrSO_3$	2.0% (wt)	14	26	23	28	7	1	2
	1.0% (wt)	15	25	21	29	7	1	2
	0.5% (wt)	18	27	19	28	4	1	3
Me_3NSO_3	2.0% (wt)	25	20	23	28	2	0	2
	1.0% (wt)	33	23	19	22	2	0	2
	0.5% (wt)	20	37	5	37	0	0	1
Et_3NSO_3	2.0% (wt)	20	30	17	28	2	0	2
	1.0% (wt)	22	30	16	28	2	0	2
	0.5% (wt)	20	32	14	31	1	0	2

the shoulder systematically increases from 5 $mAh.g^{-1}$ to 30 $mAh.g^{-1}$ as the concentration of the additive in the electrolyte is increased (Figure 3a). The additive reduction allows Li^+ insertion into the graphite electrode and prevents further decomposition of the carbonate solvents. Excellent reversibility toward Li^+ insertion/extraction of graphite is also achieved with 84.7%, 87.9%, and 91.7% coulombic efficiency for electrolytes with $PyrSO_3$ concentrations of 2.0% (wt), 1.0% (wt), and 0.5% (wt), respectively.

A clear reduction plateau is not observed with added Me_3NSO_3 or Et_3NSO_3. Nevertheless, insertion of Li^+ is observed at lower potential upon addition of 1.0% or 2.0% Me_3NSO_3 (Figure 3b). All three concentrations of Et_3NSO_3 (0.5%, 1.0%, and 2.0%) afford intercalation of Li^+ into graphite reaching its full capacity at 0.005 V vs. Li/Li^+ (Figure 3c). Upon passivation of graphite, excellent coulombic efficiency is observed, 92.9% and 93.5% with 1.0% and 2.0% added Me_3NSO_3, respectively, and 93.4%, 93.7%, and 93.5% with 0.5%, 1.0%, and 2.0% added Et_3NSO_3.

Since incorporation of added $PyrSO_3$, Me_3NSO_3, or Et_3NSO_3 affords reversible cycling of graphite electrodes with PC based electrolytes, electrochemical cycling with graphite/$LiNi_{0.5}Mn_{1.5}O_4$ cells has been further investigated, as described below.

Surface analysis by XPS.—Graphite electrodes cycled once at the C/20 rate in half-cells at 25°C (Figure 3) have been analyzed with XPS analysis to develop a better understanding of the role of the additive in SEI formation on the graphite anode. The graphite electrodes have been analyzed in the delithiated state. Relative atomic concentration of selected elements present at the surface of the graphite electrodes is displayed in Table I and the C 1 s, S 2p, and N 1s element spectra are provided in Figures 4, 5, and 6, respectively.

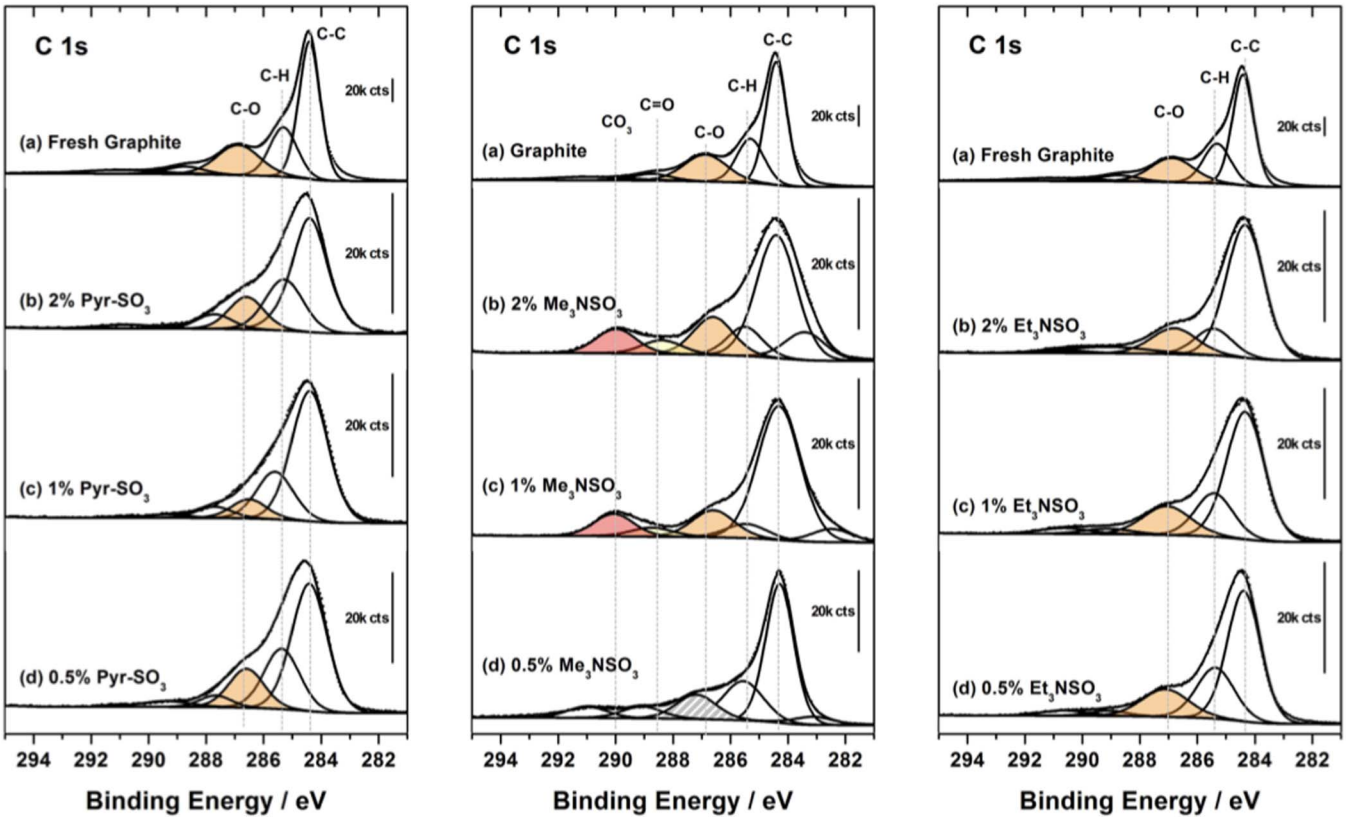

Figure 4. C 1s core spectra of the (a) fresh graphite and (b, c, d) graphite electrodes after one cycle in graphite/Li half-cells at 25°C in the PC/EMC (1/1 vol.) 1 M $LiPF_6$ electrolyte comprising (on the right) the $PyrSO_3$ additive at concentrations of (b) 2.0% (wt), (c) 1.0% (wt), and (d) 0.5% (wt), (on the center) Me_3NSO_3 at concentrations of (b) 2.0% (wt) and (c) 1.0% (wt); (on the right) Et_3NSO_3 at concentrations of (b) 2.0% (wt) and (c) 1.0% (wt), and (d) 0.5% (wt).

Downloaded on 2019-04-18 to IP 131.128.197.122 address. Redistribution subject to ECS terms of use (see ecsdl.org/site/terms_use) unless CC License in place (see abstract).

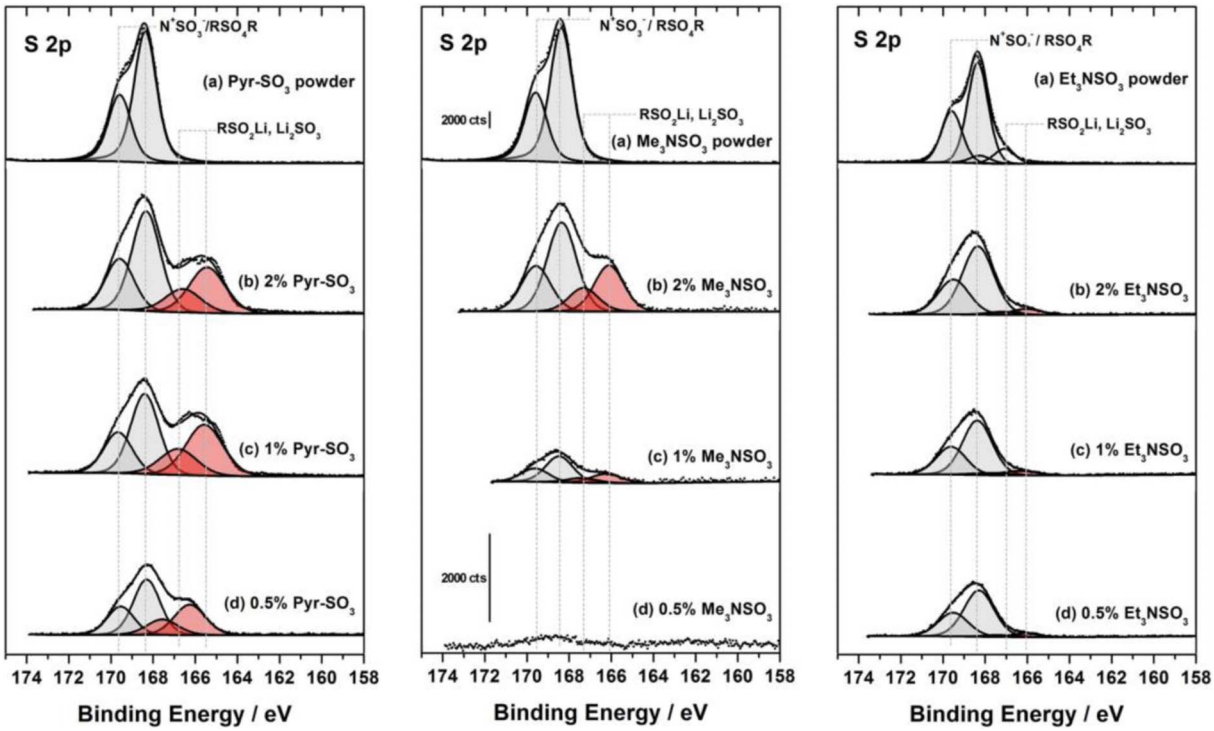

Figure 5. S 2p core spectra of the (a) $PyrSO_3$, Me_3NSO_3, Et_3NSO_3 powders and graphite electrodes after one cycle in graphite/Li half-cells at 25°C in the PC/EMC (1/1 vol.) 1 M $LiPF_6$ electrolyte comprising (on the right) the $PyrSO_3$ additive at concentrations of (b) 2.0% (wt), (c) 1.0% (wt), and (d) 0.5% (wt), (on the center) Me_3NSO_3 at concentrations of (b) 2.0% (wt) and (c) 1.0% (wt); (on the right) Et_3NSO_3 at concentrations of (b) 2.0% (wt) and (c) 1.0% (wt), and (d) 0.5% (wt).

The fresh graphite electrode contains a high concentration of C from the graphite anodes and a low concentration of O from the CMC/SBR binder and surface contamination of the graphite. All of the graphite electrodes cycled with electrolyte containing added $PyrSO_3$ have similar concentrations of F, Li, N, and P. On the contrary, small variations in the concentrations of C, O, and S are observed for the electrodes cycled with electrolyte containing 2%, 1%, and 0.5% $PyrSO_3$. As the additive concentration increases, the concentration of C is decreased and the concentration of O and S are increased. This suggests that the decomposition products of $PyrSO_3$ are incorporated into the SEI on the graphite anode. The graphite electrodes cycled with added Me_3NSO_3 or Et_3NSO_3 have variable concentrations of C, F, and O as a function of additive concentration. However, the presence of S along with the reversible cycling of the PC based electrolyte suggests that incorporation of the SO_3 additives alter the structure of the SEI on the graphite electrodes.

The C 1s spectra of the graphitic anodes cycled with electrolyte containing 2.0%, 1.0%, and 0.5% of added SO_3 complex are presented in Figure 4, along with the fresh graphite electrode. For the composite graphite electrode (4a), characteristic peaks of C-C (284.3 eV), C-H (285.6 eV), and C-O (286.5 eV) are observed and are dominated by the C-C peak.[27,28] Similar C 1s peaks are observed at 284.3 eV (C-C), 285.6 eV (C-H), and 286.5 eV (C-O), with comparable intensities for graphite electrodes cycled with electrolyte containing all three concentrations of added $PyrSO_3$ (Figures 4b, 4c, and 4d, on the left). Interestingly, there are no peaks observed at 290 eV characteristic of Li_2CO_3 or lithium alkyl carbonates form carbonate solvent reduction observed for any of the graphite electrodes cycled with $PyrSO_3$.[28] Thus, additive decomposition appears to suppress PC/EMC reduction and allows reversible cycling of graphite, in a PC-based electrolyte.

Similar trends are observed for the C1s spectra of electrodes cycled with electrolytes containing added Me_3NSO_3 or Et_3NSO_3. The C 1s spectrum of graphite cycled in 0.5% Me_3NSO_3 is very similar to the one of fresh graphite (4, a and d), despite continuous electrolyte reduction on the anode during charging suggesting that the generation of soluble non-passivating reduction products are removed during electrode rinsing. When reversible cycling of graphite is observed at concentrations of 2.0% (Figure 4b) or 1.0% Me_3NSO_3 (Figure 4c), the C 1s spectra of the cycled electrodes contain low concentrations of peaks characteristic of CO_3 at 290 eV (Figures 4b and 4c) consistent with the presence of low concentrations of lithium alkyl carbonates or Li_2CO_3 incorporated into the SEI. The C 1s spectra of the anodes cycled with electrolyte containing added Et_3NSO_3 are very similar to those observed for the electrodes cycled with electrolytes containing $PyrSO_3$.

For all three additives, O 1s spectra of the graphite electrodes show a broad peak of oxygenated species in the 536 eV-530 eV binding energy range, as well as a predominant peak of LiF (685 eV) in the three F 1s spectra (not shown here).

All the S 2p spectra of the graphite electrodes cycled in the $PyrSO_3$-based electrolytes exhibit the main doublet of $N^+SO_3^-/RSO_3Li$ at 168.3 eV (Figure 5, on the left), consistent with the generation of lithium alkyl sulfonates, as previously reported for electrolytes containing PS.[19,20] Furthermore, intensities of the S 2p spectra increase with increasing concentration of the $PyrSO_3$ additive in the electrolyte. The S 2p spectra also include an S 2p doublet of RSO_2Li and Li_2SO_3 at 166.2 eV, which results from the further reduction of the SO_3 complexes on the lithiated graphite surface.[29,30] Similar trends are observed for the S 2p spectra of graphite electrodes cycled with electrolyte containing added Me_3NSO_3 and Et_3NSO_3. The S 2p peak intensity increases for the graphite electrodes cycled with either Me_3NSO_3 or Et_3NSO_3 as the additive concentration in the electrolyte increases (Figure 5). Although at a low concentration of Me_3NSO_3 (0.5%) continuous electrolyte reduction is observed and no S is observed on the surface, consistent with the importance of the SO_3 reduction products in the formation of a stable SEI.

The reactivity of the $PyrSO_3$ complex at low potential is also supported by the N 1s core spectra of graphite electrodes depicted in Figure 6. Distinct N 1s peaks are observed for the graphite electrodes cycled with the $PyrSO_3$-based electrolyte, consistent with the

Downloaded on 2019-04-18 to IP 131.128.197.122 address. Redistribution subject to ECS terms of use (see ecsdl.org/site/terms_use) unless CC License in place (see abstract).

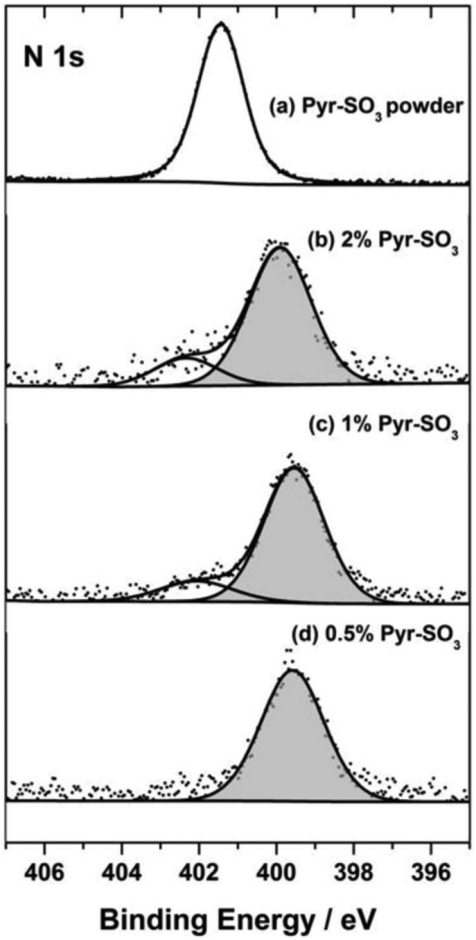

Figure 6. N 1s core spectra of the (a) $PyrSO_3$ powder and graphite electrodes after one cycle in graphite/Li half-cells at 25°C in the PC/EMC (1/1 vol.) 1 M $LiPF_6$ electrolyte comprising the $PyrSO_3$ additive at concentrations of (b) 2.0% (wt), (c) 1.0% (wt), and (d) 0.5% (wt).

highest reactivity of the $PyrSO_3$ additives in graphite half-cells (Figure 6). While a single pyridine peak is observed at 401 eV for the pure additive powder, the cycled electrodes contain a new peak at 399 eV consistent with the presence of pyridinium species.[31,32] The N 1s peak intensity is lower for all the graphite electrodes cycled with Me_3NSO_3 or Et_3NSO_3, which may result from lower reactivity or higher solubility of the amine reduction products compared to the pyridine reduction products.

Incorporation of SO_3 complexes into PC based electrolytes results in passivation of the graphite surface, which allows reversible cycling. The XPS analysis suggests that the passivating surface layers are composed of sulfur containing species and the predominant decomposition product of $LiPF_6$ (LiF). The C 1s core spectra of electrodes suggest that the S containing passivation film significantly reduces carbonate solvent reduction on the graphite surface.

$LiNi_{0.5}Mn_{1.5}O_4$/Graphite cells in PC-based electrolytes.—*Cycling performance.*—While incorporation of SO_3 complexes into PC based electrolytes for lithium ion batteries clearly leads to modification of the graphite SEI and improved cycling performance, there is also significant interest in the use of high voltage cathode materials including, $LiNi_{0.5}Mn_{1.5}O_4$. Thus, the incorporation of SO_3 complexes into graphite/high voltage spinel cells (Gr/$LiNi_{0.5}Mn_{1.5}O_4$) has been conducted to probe oxidation of the additives on the cathode to generate cathode passivation films. The cycle voltage profiles, capacity retention and coulombic efficiency for PC electrolytes with added $PyrSO_3$, Me_3NSO_3 and Et_3NSO_3 are provided in Figure 7 and Figure 8.

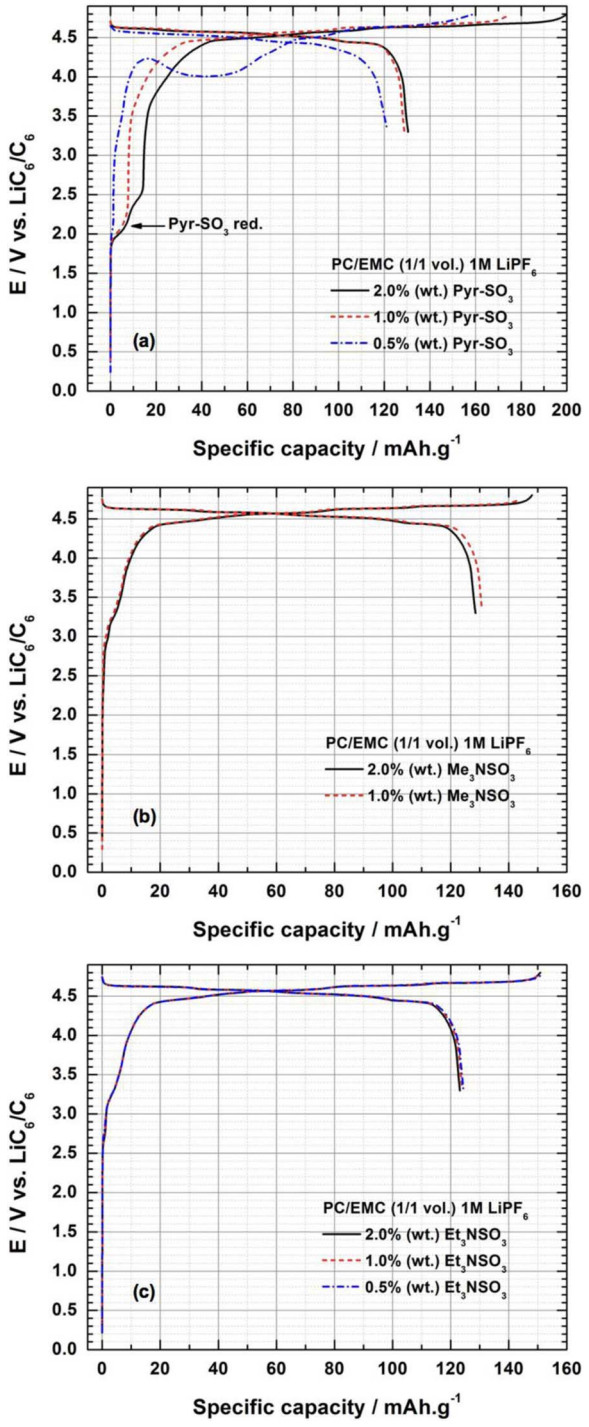

Figure 7. First cycle voltage profile of $LiNi_{0.5}Mn_{1.5}O_4$/Gr cells at 25°C (C/20 D/20, cutoff limits: 4.80 V–3.30 V vs. LiC_6/C_6) using PC/EMC (1/1 vol.) $LiPF_6$ 1 M as the baseline electrolyte with the (a) $PyrSO_3$, (b) Me_3NSO_3, and (c) Et_3NSO_3 additives (concentrations of 2.0%, 1.0%, and 0.5% (wt)).

As seen from Figure 7a, $PyrSO_3$ reduction is observed on graphite between 2.0 V–2.5 V vs. LiC_6/C_6, as discussed above for Gr/Li cells (Figure 3). A reasonable discharge capacity of ca. 130 $mAh.g^{-1}$ is observed with either 1.0 or 2.0% of added $PyrSO_3$. The first cycle coulombic efficiencies are somewhat low at 64.8% and 73.4%, respectively. The low values of efficiency are likely due to a combination of electrolyte reduction on the anode to form the SEI and electrolyte

Downloaded on 2019-04-18 to IP 131.128.197.122 address. Redistribution subject to ECS terms of use (see ecsdl.org/site/terms_use) unless CC License in place (see abstract).

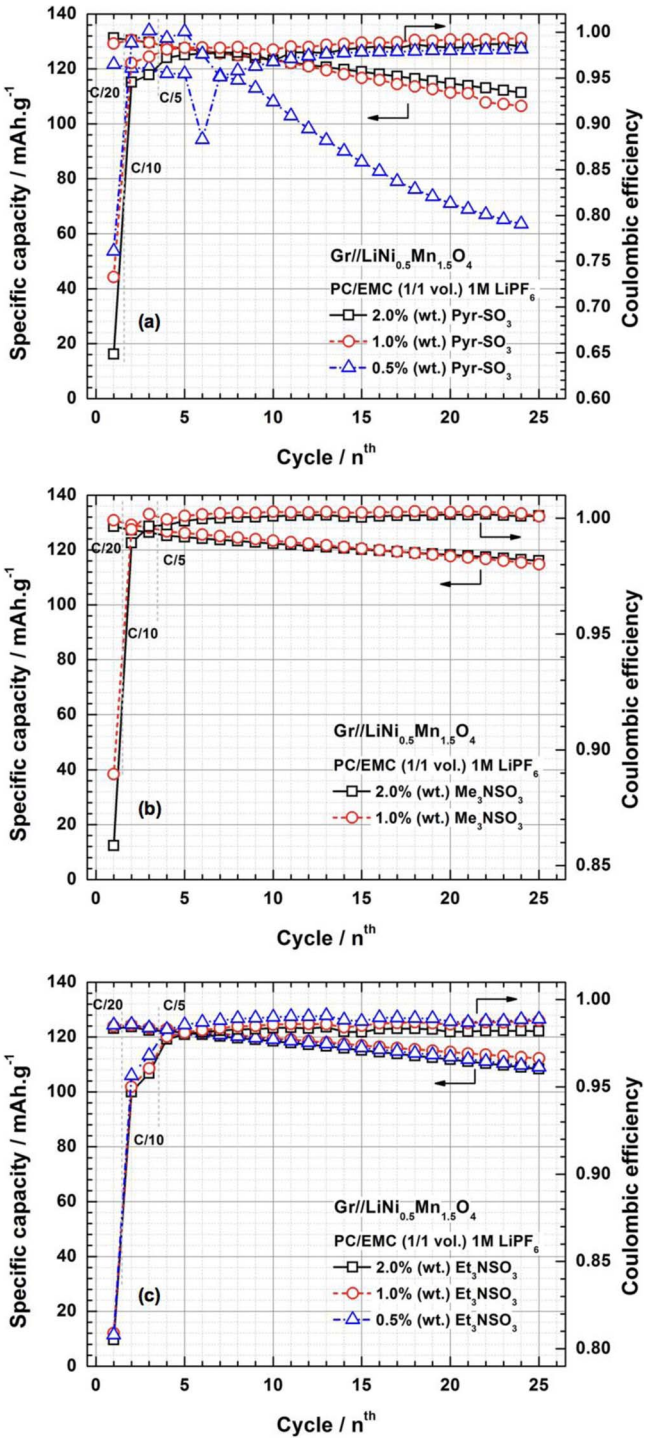

Figure 8. Cycling retention of $LiNi_{0.5}Mn_{1.5}O_4$/Graphite cells (C/5 D/5, cutoff potentials at 25°C: 4.80 V–3.30 V vs. LiC_6/C_6) using the PC/EMC (1/1 vol.) 1 M $LiPF_6$ electrolyte, which contains the (a) Me_3NSO_3 and (b) Et_3NSO_3 additives.

oxidation on the cathode surface at high voltage.[33,34] At lower concentrations of $PyrSO_3$ (0.5%), the additive does not afford good first cycle performance for $LiNi_{0.5}Mn_{1.5}O_4$/Gr cells. The first charge voltage profile contains a drop in potential from 4.3 V to 3.9 V consistent with decomposition of the electrolyte and cycling instability as discussed below (Figure 7a).

The voltage profiles during the first cycle at C/20 for cells containing electrolyte with added Me_3NSO_3 or Et_3NSO_3 are presented in Figures 7b and 7c, respectively. The profiles have a similar shape, with comparable charge capacity, which is independent of the additive concentration (ca. 150 $mAh.g^{-1}$). A plateau is observed at 3.25 V vs. LiC_6/C_6 attributed to the reduction of Me_3NSO_3 or Et_3NSO_3 on the graphite electrode (Figures 7b and 7c). However, the discharge capacities, do not depend on additive concentration but are slightly lower with added Et_3NSO_3 (ca. 123 $mAh.g^{-1}$) compared to Me_3NSO_3 (ca. 130 $mAh.g^{-1}$). The difference in behavior is not observed for Gr/Li cells suggesting the different amine SO_3 complexes have different reactivity toward the high voltage spinel.

Cycling performance at 25°C for the first 25 cycles of $LiNi_{0.5}Mn_{1.5}O_4$/Gr cells with PC based electrolytes with added SO_3 complexes is presented in Figure 8. Cycling performance of full cells with added $PyrSO_3$ is displayed in Figure 8a. Good capacity retention and efficiency are observed at higher concentrations of $PyrSO_3$ (2.0% and 1.0%) with 85% and 82% capacity retention after 25 cycles and over 99% coulombic efficiency for the final 10 cycles. However, significant capacity loss (47.7%) is obtained for cells containing 0.5% of $PyrSO_3$. The poor cycling performance is likely due to poor passivation of graphite (Figure 7a).

Cells containing electrolyte with 1% or 2% of added Me_3NSO_3 have better capacity retention, 90% and 88%, respectively (Figure 8b). The coulombic efficiency is also found to be excellent, 99.9%. Cells containing electrolyte with added Et_3NSO_3 also show good capacity retention (88–91%) and high efficiency (> 98%) for all additive concentrations. Thus, superior cycleability of cells containing either the Me_3NSO_3 complex or the Et_3NSO_3 complex is observed in high voltage $LiNi_{0.5}Mn_{1.5}O_4$/Gr cells, in agreement with that observed in graphite/Li cells. Ex-situ surface analysis of the electrodes has been conducted in order to develop a better understanding of the source of the performance enhancement of added SO_3 complexes.

Surface analysis by XPS.—$LiNi_{0.5}Mn_{1.5}O_4$ cathodes.—Surface analysis of the cathodes extracted from graphite/$LiNi_{0.5}Mn_{1.5}O_4$ cells after 25 cycles at 25°C has been conducted by XPS. The $LiNi_{0.5}Mn_{1.5}O_4$ electrodes are analyzed in the lithiated state (0% SOC). Relative atomic concentrations present on the surface of the high voltage spinel electrodes are provided in Table II.

The fresh LNMO electrode shows a high concentration of C, O, Mn, and F from the oxide particles and the PVdF binder. For the cathodes cycled with electrolyte containing added $PyrSO_3$, two types of behaviors are observed depending on the additive concentration, which relates to the cycling performance discussed above (Figure 8). For the cathodes cycled with electrolyte containing 1–2% $PyrSO_3$, similar concentrations of elements are found, while differences are observed with 0.5% $PyrSO_3$. The relative concentration of C is decreased and the concentration of O is increased consistent with lower concentrations of $PyrSO_3$ and less passivation of the cathode surface. The thinner surface films with low concentrations of $PyrSO_3$ correlate with the poor cycling performance. The cathodes cycled with electrolyte containing added Me_3NSO_3 or Et_3NSO_3 have very similar element concentrations for all concentrations investigated. Cells with all concentrations of added Me_3NSO_3 or Et_3NSO_3 have good cycling performance that the thin surface films correlate with good cycling performance (Figure 8). The results suggest that the presence of the aromatic pyridyl group may lead to higher reactivity of the cathode surface and thicker surface films, but the presence of the amines leads to thinner but more effective passivation layers on the cathode.

The O 1s spectra of cathodes cycled with electrolyte containing $PyrSO_3$, Me_3NSO_3, and Et_3NSO_3 are depicted in Figure 9. The cathodes cycled with the $PyrSO_3$ additive have a weak O-M peak at 529 eV consistent with the presence of a thick cathode surface film covering the metal oxide particles.[35,36] The O 1s spectrum is dominated by a broad peak centered at 532 eV characteristic of C-O, C = O, and S-O containing species from the reaction of the electrolyte. The cathodes cycled with Me_3NSO_3 and Et_3NSO_3 additives have much stronger O-M peaks at 529 eV and a weaker broad peak associated with electrolyte decomposition at 532 eV consistent with a thinner cathode surface film. Interestingly, the intensity of the M-O peak is in agreement with the elemental concentration data, suggesting that the

Downloaded on 2019-04-18 to IP 131.128.197.122 address. Redistribution subject to ECS terms of use (see ecsdl.org/site/terms_use) unless CC License in place (see abstract).

Table II. Relative atomic percentage (%) of selected elements at the surface of the $LiNi_{0.5}Mn_{1.5}O_4$ electrodes after cycling in $LiNi_{0.5}Mn_{1.5}O_4$/Gr cells at 25°C.

Additive concentration		C 1s	F 1s	O 1s	Mn 2p	S 2p	N 1s	P 2p
Fresh LNMO		39	15	9	37	-	-	-
$PyrSO_3$	2.0% (wt)	39	27	22	1	3	4	4
	1.0% (wt)	40	25	22	1	2	5	5
	0.5% (wt)	28	27	30	2	0	1	12
Me_3NSO_3	2.0% (wt)	52	22	19	3	1	1	2
	1.0% (wt)	49	22	20	3	1	1	3
Et_3NSO_3	2.0% (wt)	50	23	20	3	1	1	3
	1.0% (wt)	48	22	22	5	1	1	3
	0.5% (wt)	49	22	21	3	1	1	3

cathode surface film thickness is largely independent of the concentration of added Me_3NSO_3 or Et_3NSO_3.

C 1s spectra of the $LiNi_{0.5}Mn_{1.5}O_4$ cathodes are presented in Figure 10. The fresh (uncycled) cathode (Figure 10a) contains peaks characteristic of conductive carbon (284.3 eV) and the PVdF binder (-CH_2- at 286.5 eV and -CF_2- at 290.7 eV).[36,37] The cathodes cycled in the $PyrSO_3$-containing electrolytes reveal significant quantities of electrolyte decomposition on the surface. Upon incorporation of 1–2% $PyrSO_3$ new peaks characteristic of C-H (286.5 eV), C-O (286.5 eV), and CO_3 (290 eV) are observed, while the C-C peak at 284.3 eV is diminished and the CF_2 (PVdF) peak at 290.7 eV is no longer observable. The electrode cycled with 0.5% $PyrSO_3$ has only C-C (284.3 eV), CH_2 (285.6 eV), C=O (287.7 eV) and CO_3 (290 eV) observable.[35,36,38] The small contribution of the C-C peak and significant concentration of C-O and C=O peaks suggests a significant coverage of the cathode material by decomposition products of the electrolyte, consistent with the intensities of the O-M peak in the O 1s spectra. The $LiNi_{0.5}Mn_{1.5}O_4$ cathodes cycled with electrolyte containing either Me_3NSO_3 or Et_3NSO_3 are different that those cycled with $PyrSO_3$. The C-C (284.3 eV), CH_2 (286.5 eV) and CF_2 (290.7 eV) peaks of the PVdF binder are weak, but visible, suggesting thinner passive layers. Nevertheless, the CEI of these cathodes contains the C-O (286.5 eV), C=O (287.7 eV), and CO_3 (290 eV) functional groups coming from PC and EMC oxidation. As previously observed from the O 1s spectra, the C 1s spectra are very similar for all additive concentrations. The surface chemistry of the cathode surface layers does not depend on the additive concentration in the baseline electrolyte.

The S 2p spectra of the cathodes are depicted in Figure 11. For the cathodes cycled with $PyrSO_3$ are dominated by the doublet of peaks characteristic of $N^+SO_3^-$/RSO_3Li. An additional minor doublet of peaks characteristic of S-S species appears at 164 eV.[39-41] The presence of S on the surface suggests participation of the sulfonate in the CEI (Cathode Electrolyte Interface). When the concentration of

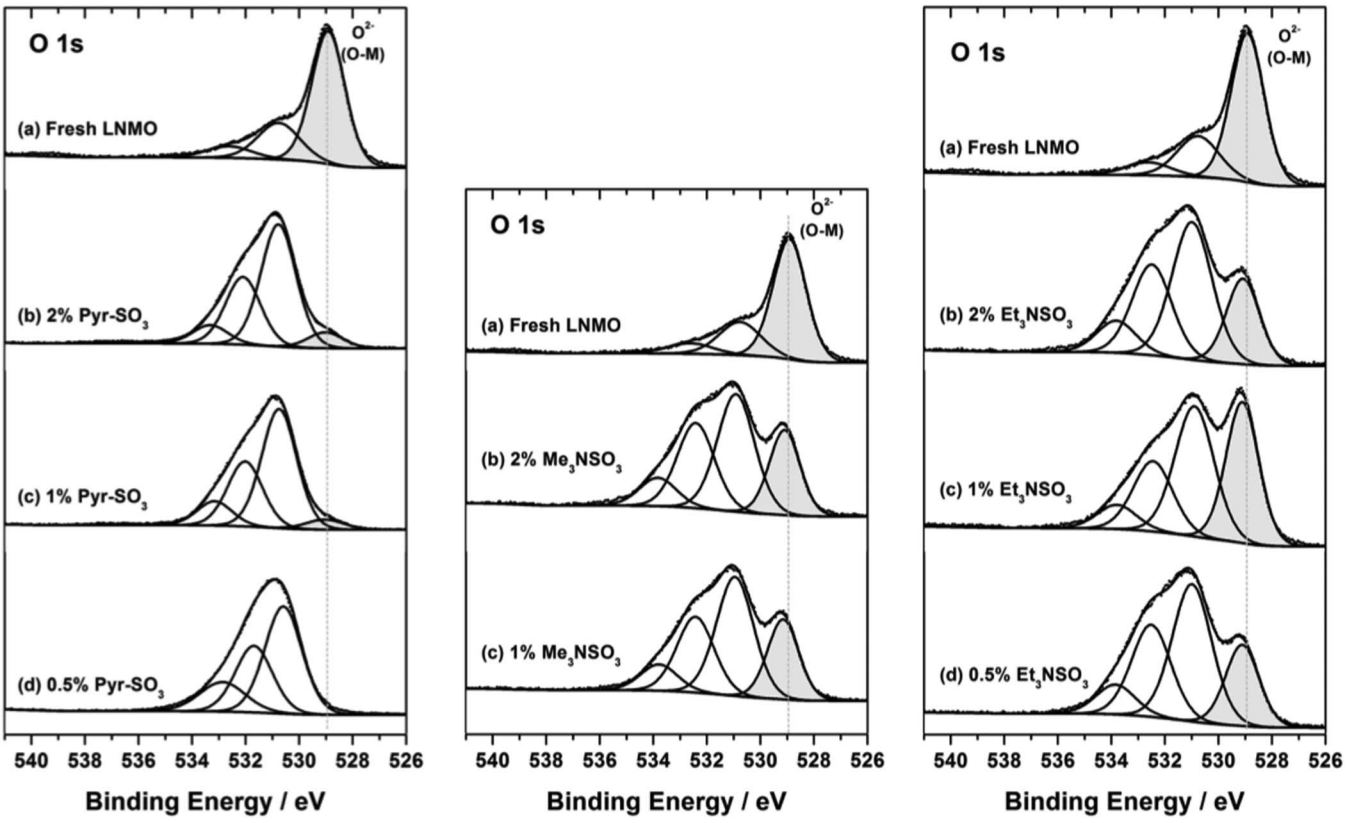

Figure 9. O 1s core spectra of (a) the $LiNi_{0.5}Mn_{1.5}O_4$ fresh electrode and $LiNi_{0.5}Mn_{1.5}O_4$ cathodes cycled with graphite in the PC/EMC (1/1 vol.) 1 M $LiPF_6$ electrolyte comprising (on the right) the $PyrSO_3$ additive at concentrations of (b) 2.0% (wt), (c) 1.0% (wt), and (d) 0.5% (wt), (on the center) the Me_3NSO_3 additive at concentrations of (b) 2.0% (wt), (c) 1.0% (wt), and (on the left) Et_3NSO_3 at concentrations of (b) 2.0% (wt), (c) 1.0% (wt), and (d) 0.5% (wt).

Downloaded on 2019-04-18 to IP 131.128.197.122 address. Redistribution subject to ECS terms of use (see ecsdl.org/site/terms_use) unless CC License in place (see abstract).

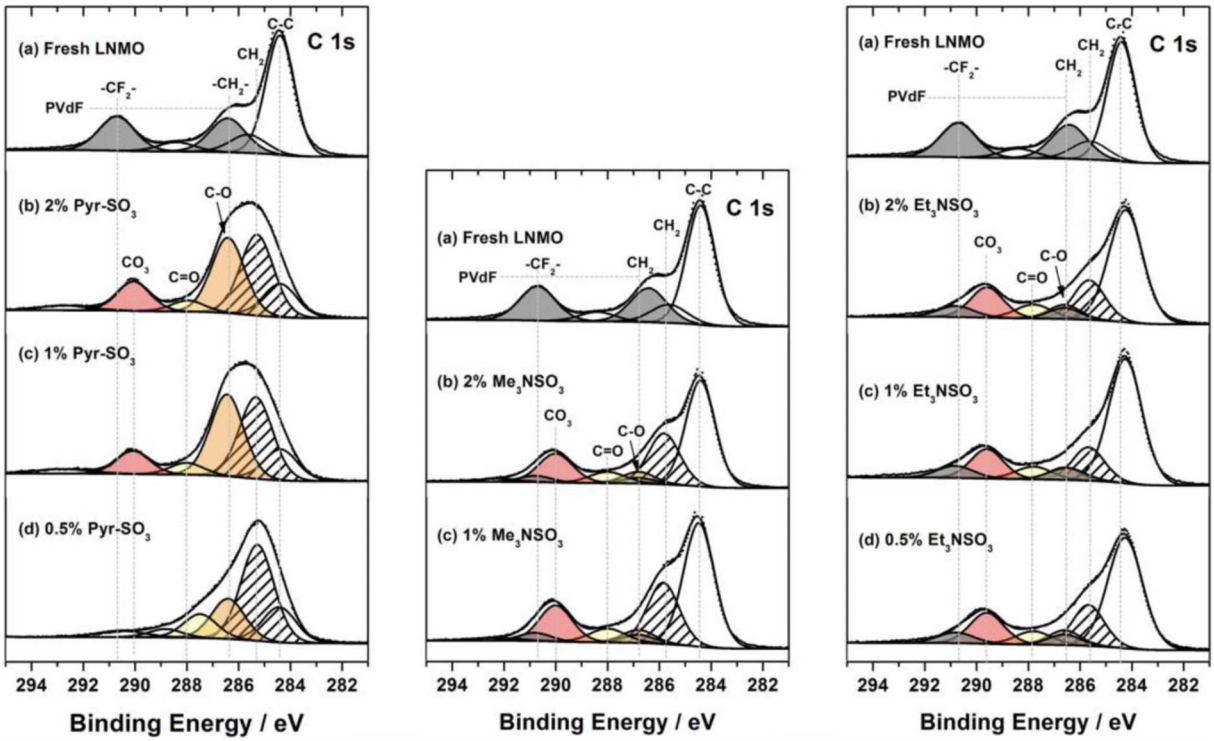

Figure 10. C 1s core spectra of (a) the $LiNi_{0.5}Mn_{1.5}O_4$ fresh electrode and $LiNi_{0.5}Mn_{1.5}O_4$ cathodes cycled with graphite in the PC/EMC (1/1 vol.) 1 M $LiPF_6$ electrolyte comprising (on the right) the $PyrSO_3$ additive at concentrations of (b) 2.0% (wt), (c) 1.0% (wt), and (d) 0.5% (wt), (on the center) the Me_3NSO_3 additive at concentrations of (b) 2.0% (wt), (c) 1.0% (wt), and (on the left) Et_3NSO_3 at concentrations of (b) 2.0% (wt), (c) 1.0% (wt), and (d) 0.5% (wt).

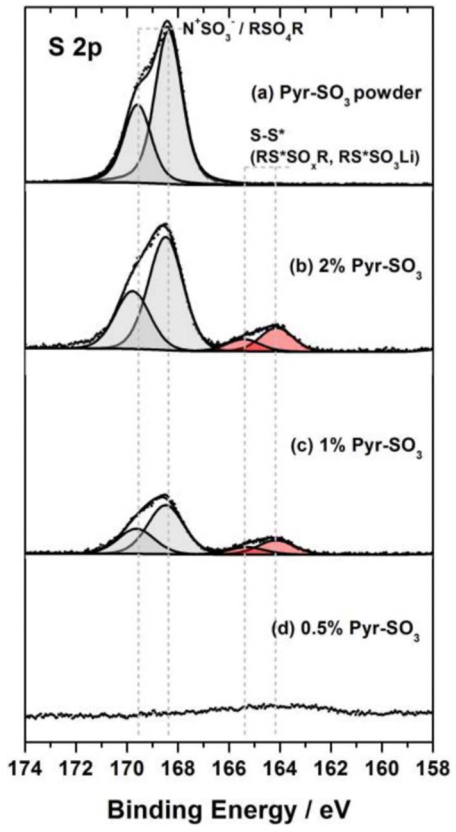

Figure 11. S 2p core spectra of (a) the $PyrSO_3$ powder and $LiNi_{0.5}Mn_{1.5}O_4$ cathodes cycled with graphite in the PC/EMC (1/1 vol.) 1 M $LiPF_6$ electrolyte comprising the $PyrSO_3$ additive at concentrations of (b) 2.0% (wt), (c) 1.0% (wt), and (d) 0.5% (wt).

$PyrSO_3$ is reduced to 0.5%, no sulfur is detected on the $LiNi_{0.5}Mn_{1.5}O_4$ surface. The concentration of S on the surface of electrodes cycled with electrolyte containing either Me_3NSO_3 or Et_3NSO_3 is very low for all additive concentrations, consistent with thin cathode surface films as discussed above.

To conclude, two types of CEIs are observed on the $LiNi_{0.5}Mn_{1.5}O_4$ cathode depending on the additive structure. For the $PyrSO_3$ electrolytes, significant electrolyte decomposition is observed via the O 1s and C 1s spectra. This results in the generation of a thick passive layer which contains S. Alternatively, incorporation of Me_3NSO_3 and Et_3NSO_3 additives results in a thin, but passivating CEI. Consequently, better cycling retention and higher coulombic efficiency are observed for PC/EMC electrolytes with added Me_3NSO_3 and Et_3NSO_3.

The graphite anodes extracted from graphite/$LiNi_{0.5}Mn_{1.5}O_4$ cells cycled with PC based electrolyte with added SO_3 complexes were also analyzed by XPS. The surface species are relatively similar to those observed on the graphite electrodes extracted from Li/graphite cells and are not presented here.

Conclusions

An investigation of novel bifunctional additives $PyrSO_3$, Me_3NSO_3 and Et_3NSO_3 has been conducted. In order to develop an understanding of the role of SO_3 additives in anode SEI formation and stability, PC based electrolytes with and without added SO_3 complexes have been conducted. Incorporation of any of the SO_3 complexes, $PyrSO_3$, Me_3NSO_3 and Et_3NSO_3, result in the generation of a stable SEI on the graphite electrodes allowing reversible cycling with high coulombic efficiency with the PC-based electrolyte. The SO_3 complexes are reduced at low potential into sulfates and sulfites, as evidenced by XPS analysis, which results in an efficient passivation layer on the graphite. The compatibility of the SO_3 additives with high voltage cathodes has also been probed. Excellent cycling performance of $LiNi_{0.5}Mn_{1.5}O_4$/Gr cell has been obtained with the same PC-based electrolyte with added Me_3NSO_3 or Et_3NSO_3.

Downloaded on 2019-04-18 to IP 131.128.197.122 address. Redistribution subject to ECS terms of use (see ecsdl.org/site/terms_use) unless CC License in place (see abstract).

Incorporation of Me_3NSO_3 and Et_3NSO_3 results in a thin but stable cathode passivation layer on the $LiNi_{0.5}Mn_{1.5}O_4$ oxide particles resulting in good cyclability and coulombic efficiency.

Acknowledgment

The authors thank BASF SE Electrochemistry Research Network for financial support.

References

1. K. Xu, *Chemical reviews*, **114**, 11503 (2014).
2. K. Xu, *Chemical reviews*, **104**, 4303 (2004).
3. M. Nie and B. L. Lucht, *Journal of The Electrochemical Society*, **161**, A1001 (2014).
4. R. Petibon, J. Xia, L. Ma, M. K. G. Bauer, K. J. Nelson, and J. R. Dahn, *Journal of The Electrochemical Society*, **163**, A2571 (2016).
5. J. Xia, R. Petibon, D. Xiong, L. Ma, and J. R. Dahn, *Journal of Power Sources*, **328**, 124 (2016).
6. S. S. Zhang, *Journal of Power Sources*, **162**, 1379 (2006).
7. K. Abe, in *Electrolytes for Lithium and Lithium Ion Batteries*, Richard T Jow, Kang Xu, Oleg Borodin, and M. Ue, Editors, Springer-Verlag New York (2014).
8. Y. Ein-Eli, S. R. Thomas, and V. R. Koch, *Journal of The Electrochemical Society*, **143**, L195 (1996).
9. Y. Ein-Eli, S. R. Thomas, and V. R. Koch, *Journal of The Electrochemical Society*, **144**, 1159 (1997).
10. Y. Ein-Eli, *Journal of Electroanalytical Chemistry*, **531**, 95 (2002).
11. J. O. Besenhard, M. W. Wagner, M. Winter, A. D. Jannakoudakis, P. D. Jannakoudakis, and E. Theodoridou, *Journal of Power Sources*, **44**, 413 (1993).
12. M. W. Wagner, C. Liebenow, and J. O. Besenhard, *Journal of Power Sources*, **68**, 328 (1997).
13. G. H. Wrodnigg, J. O. Besenhard, and M. Winter, *Journal of The Electrochemical Society*, **146**, 470 (1999).
14. G. H. Wrodnigg, J. O. Besenhard, and M. Winter, *Journal of Power Sources*, **97–98**, 592 (2001).
15. B. Li, M. Xu, T. Li, W. Li, and S. Hu, *Electrochemistry Communications*, **17**, 92 (2012).
16. M. Q. Xu, W. S. Li, X. X. Zuo, J. S. Liu, and X. Xu, *Journal of Power Sources*, **174**, 705 (2007).
17. R. Wagner, S. Brox, J. Kasnatscheew, D. R. Gallus, M. Amereller, I. Cekic-Laskovic, and M. Winter, *Electrochemistry Communications*, **40**, 80 (2014).
18. J. Xia, N. N. Sinha, L. P. Chen, and J. R. Dahn, *Journal of the Electrochemical Society*, **161**, A264 (2013).
19. M. Xu, W. Li, and B. L. Lucht, *Journal of Power Sources*, **193**, 804 (2009).
20. B. Zhang, M. Metzger, S. Solchenbach, M. Payne, S. Meini, H. A. Gasteiger, A. Garsuch, and B. L. Lucht, *The Journal of Physical Chemistry C*, **119**, 11337 (2015).
21. M. Xu, L. Zhou, Y. Dong, Y. Chen, J. Demeaux, A. D. MacIntosh, A. Garsuch, and B. L. Lucht, *Energy & Environmental Science*, **9**, 1308 (2016).
22. M. Nie,L. Ma, J. Xia, A. Xiao, W. M. Lamanna, K. Smith, and J. R. Dahn, *Journal of The Electrochemical Society*, **163**, A2124 (2016).
23. C. L. Campion, W. Li, and B. L. Lucht, *Journal of The Electrochemical Society*, **152**, A2327 (2005).
24. M. J. Frisch, G. W. Trucks, H. B. Schlegel, G. E. Scuseria, M. A. Robb, J. R. Cheeseman, J. A. Montgomery, T. Vreven, K. N. Kudin, J. C. Burant, J. M. Millam, S. S. Iyengar, J. Tomasi, V. Barone, B. Mennucci, M. Cossi, G. Scalmani, N. Rega, G. A. Petersson, H. Nakatsuji, M. Hada, M. Ehara, K. Toyota, R. Fukuda, J. Hasegawa, M. Ishida, T. Nakajima, Y. Honda, O. Kitao, H. Nakai, M. Klene, X. Li, J. E. Knox, H. P. Hratchian, J. B. Cross, V. Bakken, C. Adamo, J. Jaramillo, R. Gomperts, R. E. Stratmann, O. Yazyev, A. J. Austin, R. Cammi, C. Pomelli, J. W. Ochterski, P. Y. Ayala, K. Morokuma, G. A. Voth, P. Salvador, J. J. Dannenberg, V. G. Zakrzewski, S. Dapprich, A. D. Daniels, M. C. Strain, O. Farkas, D. K. Malick, A. D. Rabuck, K. Raghavachari, J. B. Foresman, J. V. Ortiz, Q. Cui, A. G. Baboul, S. Clifford, J. Cioslowski, B. B. Stefanov, G. Liu, A. Liashenko, P. Piskorz, I. Komaromi, R. L. Martin, D. J. Fox, T. Keith, A. Laham, C. Y. Peng, A. Nanayakkara, M. Challacombe, P. M. W. Gill, B. Johnson, W. Chen, M. W. Wong, C. Gonzalez, and J. A. Pople, Gaussian 03, Revision C.02, in (2003).
25. V. A. Agubra and J. W. Fergus, *Journal of Power Sources*, **268**, 153 (2014).
26. G. C. Chung, H. J. Kim, S. I. Yu, S. H. Jun, J. w. Choi, and M. H. Kim, *Journal of The Electrochemical Society*, **147**, 4391 (2000).
27. L. Castro, R. Dedryveère, J. B. Ledeuil, J. Breéger, C. Tessier, and D. Gonbeau, *Journal of The Electrochemical Society*, **159**, A357 (2012).
28. L. Bodenes, R. Dedryvere, H. Martinez, F. Fischer, C. Tessier, and J. P. Peres, *Journal of the Electrochemical Society*, **159**, A1739 (2012).
29. N. Andreu, D. Flahaut, R. Dedryvere, M. Minvielle, H. Martinez, and D. Gonbeau, *ACS applied materials & interfaces*, **7**, 6629 (2015).
30. B. Li, M. Xu, B. Li, Y. Liu, L. Yang, W. Li, and S. Hu, *Electrochimica Acta*, **105**, 1 (2013).
31. H. Wang, C. Zhang, Z. Liu, L. Wang, P. Han, H. Xu, K. Zhang, S. Dong, J. Yao, and G. Cui, *Journal of Materials Chemistry*, **21**, 5430 (2011).
32. S. Men, D. S. Mitchell, K. R. Lovelock, and P. Licence, *Chemphyschem : a European journal of chemical physics and physical chemistry*, **16**, 2211 (2015).
33. J. Demeaux, D. Lemordant, M. Caillon-Caravanier, H. Galiano, and B. Claude-Montigny, *Electrochimica Acta*, **89**, 163 (2013).
34. J. Demeaux, D. Lemordant, H. Galiano, M. Caillon-Caravanier, and B. Claude-Montigny, *Electrochimica Acta*, **116**, 271 (2014).
35. R. Dedryveère, D. Foix, S. Franger, S. Patoux, L. Daniel, and D. Gonbeau, *The Journal of Physical Chemistry C*, **114**, 10999 (2010).
36. H. Bouayad, Z. Wang, N. Dupré, R. Dedryvère, D. Foix, S. Franger, J. F. Martin, L. Boutafa, S. Patoux, D. Gonbeau, and D. Guyomard, *The Journal of Physical Chemistry C*, **118**, 4634 (2014).
37. J. Pires, A. Castets, L. Timperman, J. Santos-Peña, E. Dumont, S. Levasseur, C. Tessier, R. Dedryvère, and M. Anouti, *Journal of Power Sources*, **296**, 413 (2015).
38. S. Malmgren, K. Ciosek, M. Hahlin, T. Gustafsson, M. Gorgoi, H. Rensmo, and K. Edström, *Electrochimica Acta*, **97**, 23 (2013).
39. L. Madec, R. Petibon, K. Tasaki, J. Xia, J. P. Sun, I. G. Hill, and J. R. Dahn, *Physical chemistry chemical physics*, **17**, 27062 (2015).
40. G. Zhou, L. -C. Yin, D. -W. Wang, L. Li, S. Pei, I. R. Gentle, F. Li, and H. -M. Cheng, *ACS Nano*, **7**, 5367 (2013).
41. R. Demir-Cakan, M. Morcrette, Gangulibabu, A. Guéguen, R. Dedryvère, and J. -M. Tarascon, *Energy & Environmental Science*, **6**, 176 (2013).

Downloaded on 2019-04-18 to IP 131.128.197.122 address. Redistribution subject to ECS terms of use (see ecsdl.org/site/terms_use) unless CC License in place (see abstract).